JCTC Journal of Chemical Theory and Computation

Article

pubs.acs.org/JCTC

Preferential Solvation of Triglycine in Aqueous Urea: An Open Boundary Simulation Approach

Debashish Mukherji

Max-Planck Institut für Polymerforschung, Ackermannweg 10, 55128 Mainz, Germany

Nico F. A. van der Vegt

Center of Smart Interfaces, Technische Universität Darmstadt, Petersenstrasse 32, 64287 Darmstadt, Germany

Kurt Kremer*

Max-Planck Institut für Polymerforschung, Ackermannweg 10, 55128 Mainz, Germany

ABSTRACT: Solvation free energies of peptides in water decrease with increasing urea concentration and therefore lead to increased solubility. In this work, we study the solvation thermodynamics of a triglycine in aqueous urea solutions at room temperature T = 300 K. We perform our analysis within the framework of the Kirkwood−Buff theory of liquid mixtures, developed for open systems. For this purpose, we use a recently proposed approach to study liquid mixtures within an "effective" open boundary simulation scheme (AdResS). We couple a small open boundary all-atom (explicit) region to a much larger coarse-grained particle reservoir. This coupling allows the free exchange of particles in thermodynamic equilibrium. Our approach preserves correct particle fluctuations that are important for studying the concentration driven conformational transition of (bio)molecules.

1. INTRODUCTION

The structure, function, and stability of proteins are intimately linked to the presence of small cosolvents within the hydration shell of the protein structures.[1−6] Thus, the overall (bio)-physical properties are usually governed by the relative interaction between a protein with cosolvents and the protein with water. One such cosolvent is urea, which is known to trigger unfolding (or denaturation) of a polypeptide, ranging from a small peptide to a more complex protein structure.[7−9] Furthermore, the molecular mechanism of protein denaturation in the presence of urea has been the subject of a long-standing debate.[10−16] Structural instabilities within a protein structure can severely affect its natural function. Therefore, it is sometime crucial to have detailed structural information, at the microscopic level, to understand global thermodynamic properties. These studies, however, are predominantly limited to the closed boundary NVT (constant number of particles, N; constant volume, V; and constant temperature, T) or NpT (constant pressure, p) simulations. However, problems may arise when the conformational transition of a protein is intimately linked to large local concentration fluctuations, leading to severe finite size effects for mid-size systems. For example, in the case of large proteins, the conformational transition usually drives a large number of urea molecules near the protein structure. The excess of urea molecules near a protein leads to depletion of urea elsewhere within the closed boundary simulation setup. Hence, it disturbs the cosolvent equilibrium with the bulk solution, which is extremely important to maintain in order to make any meaningful comparison with the experiments that are done within the osmotic conditions. This limitation can somehow be eliminated by taking enormously large system sizes, where attaining large time scales can sometimes be computationally too demanding, especially when full chemical details need to be taken into account. Therefore, it is important to use an alternative simulation scheme that can mimic local concentration fluctuations correctly. In this context, we have recently proposed an approach to simulate aqueous mixtures in an "effective" open boundary simulation scheme.[17,18] Our approach makes use of the previously developed Adaptive Resolution Scheme (AdResS).[18−22] In AdResS, particle exchange is possible, on the fly, in full thermodynamic equilibrium. We showed that by coupling a small all-atom (explicit) region with a much larger osmotic coarse-grained reservoir, the correct concentration fluctuations could be captured.[17] To calculate the concentration fluctuations, we have treated the all-atom region within the framework of the fluctuation theory of Kirkwood and Buff,[23] derived for the grand-canonical ensemble. It is yet important to mention that we could capture correct concentration fluctuations within the small all-atom (explicit) region that consisted of only 3% of the whole simulation domain,[17] suggesting a possible more efficient approach to simulate complex (bio)macromolecules.

In this work, we present an extension of our previously proposed approach,[17] and as a first step, we study the solvation of a triglycine molecule in aqueous urea solutions. We again

Special Issue: Wilfred F. van Gunsteren Festschrift

Received: March 28, 2012
Published: July 9, 2012

take a small open boundary all-atom region which is coupled to an osmotic coarse-grained reservoir. The triglycine is situated at the center of this all-atom subregion, keeping thermodynamic equilibrium with an osmotic coarse-grained reservoir. The solvation free energies are calculated within this subvolume by making use of the KB theory of solutions developed for open systems. Our analysis will predominantly focus on the investigation of the solvation thermodynamics for pure aqueous urea and for triglycine solvated in aqueous urea.

The remainder of the paper is organized as follows: In section 2, we sketch the method where we give a brief summary of the AdResS method together with the KB theory of solutions. The results are presented in section 3, and finally we give our conclusions in section 4.

2. METHODOLOGY

For the simulations, we use the single precession GROMACS molecular dynamics code.[24] The aqueous urea mixtures are simulated using the Kirkwood−Buff derived force field[25] for urea and the SPC/E water model.[26] It is yet important to mention that the specific choice of the water model does not significantly alter the thermodynamic properties of aqueous mixtures. In this context, three water models (SPC, SPC/E, and TIP3P) were tested that lead to the same results for aqueous urea.[25] We consider four different urea molar concentrations c_u, namely, 2.00 M (616 urea and 15 528 water molecules), 3.99 M (1232 urea and 14 000 water molecules), 6.00 M (1848 urea and 12 456 water molecules), 8.02 M (2464 urea and 10 896 water molecules), and 9.80 M (3080 urea and 9263 water molecules). These values of c_u correspond to 0.0382, 0.0809, 0.1292, 0.1844, and 0.2495 in the unit of urea mole fraction x_u. We restrict the concentration to below 9.80 M because urea is known to denature proteins in around 6 to 8 M solutions.[10] The force field parameters for triglycine are taken from Gromos43a1.[27] The all-atom simulations are performed in an *NpT* ensemble, where the pressure is controlled with a Berendsen barostat at 1 atm of pressure using a coupling time of 0.5 ps.[28] The temperature is set to 300 K using a Berendsen thermostat with a coupling time of 0.1 ps. The integration time step is 1 fs. Electrostatics in all-atom simulations are treated using particle mesh ewald. AdResS simulations are performed using modified GROMACS code.[29] The electrostatics for the AdResS setup are treated using the reaction field method.[29,30] The reaction field dielectric constants ϵ_r are calculated from all-atom simulation trajectories.[31] The bond lengths of the urea molecules are constrained using the LINCS algorithm.[32]

2.1. AdResS Scheme. The adaptive resolution scheme[20,21] is a multiscale approach that can couple a small region of high resolution (e.g., atomistic) molecules and a large region, which here serves as low resolution (e.g., coarse-grained) reservoir. In between, there is a "so called" hybrid region, where particles smoothly change their resolution from atomistic to coarse-grained and vice versa. This transition is governed by a weighted function $w(r) \in [0, 1]$. $w(r)$ is unity for the explicit system, zero for the coarse-grained system, and smoothly varies between zero and unity in the hybrid region. AdResS uses interpolated forces between molecules α and β

$$\mathbf{F}_{\alpha\beta} = w(r_\alpha)\, w(r_\beta)\, \mathbf{F}^{\mathrm{exp}}_{\alpha\beta} + [1 - w(r_\alpha)\, w(r_\beta)]\mathbf{F}^{\mathrm{cg}}_{\alpha\beta} \qquad (1)$$

$\mathbf{F}_{\alpha\beta}$ is the total intermolecular force acting between two molecules, and $\mathbf{F}^{\mathrm{exp}}_{\alpha\beta}$ is the sum of all high resolution pairwise interactions between atoms of molecules α and β. $\mathbf{F}^{\mathrm{cg}}_{\alpha\beta} = -\nabla V^{\mathrm{cg}}_{\alpha\beta}$ is the pairwise coarse-grained force based on $V^{\mathrm{cg}}_{\alpha\beta}$, the pairwise coarse-grained potential. r_α and r_β are the distances of the molecular centers of mass from the center of the simulation domain, see Figure 1, where we show a typical simulation setup

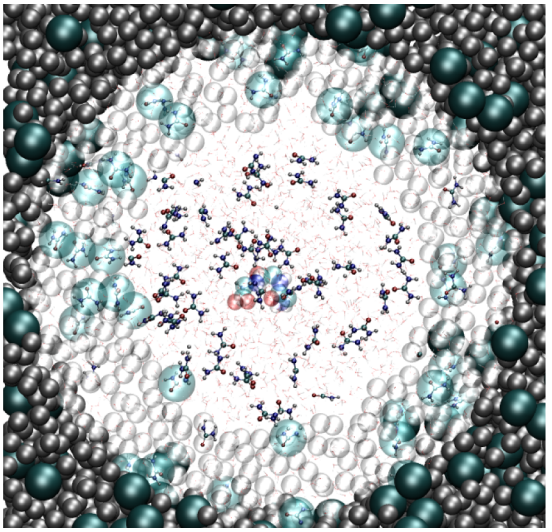

Figure 1. A typical AdResS simulation setup of triglycine solvated in an aqueous urea mixture at 2.00 M. An open boundary all-atom (explicit) region of 2 nm radius is coupled to a much larger coarse-grained bath. Coarse-grained urea beads are rendered in green, and steel is chosen for coarse-grained water.

of triglycine solvated in a 2.00 M aqueous urea solution. The molecules change their spatial resolutions (from all atom to coarse-grained and vice versa) on the fly allowing for free exchange of particles in full thermodynamic equilibrium[19,21] (for details, see the Supporting Information of ref 19). Recently, we have proposed an approach that uses this scheme to study liquid mixtures in an "effective" open boundary simulation within the framework of the Kirkwood−Buff theory of solutions.[17] In the present work, we use this approach to study the solvation thermodynamics of triglycine in aqueous urea solutions. The nonbonded pairwise potentials in the coarse-grained region are derived using the Iterative Boltzmann Inversion (IBI) method, implemented in the VOTCA package.[33] Due to the nontransferability of coarse-grained potentials with concentrations, we derive coarse-grained potentials for individual concentrations separately. In Figure 2, we show the typical IBI derived pairwise coarse-grained potential for the two different urea molar concentrations.

2.2. Fluctuation Theory: Kirkwood−Buff Integrals. Kirkwood−Buff theory[23] relates fluctuations in the grand canonical ensemble to integrals of radial distribution functions $g_{ij}(r)$ over the volume. These "so-called" Kirkwood−Buff integrals (KBI) are related to thermodynamic properties of mixtures, as given in eq 2. For solution components i and j, these KBIs are defined as[23]

$$G_{ij} = V\left[\frac{\langle N_i N_j\rangle - \langle N_i\rangle\langle N_j\rangle}{\langle N_i\rangle\langle N_j\rangle} - \frac{\delta_{ij}}{\langle N_j\rangle}\right] = 4\pi\int_0^\infty [g_{ij}^{\mu VT}(r) - 1]r^2\, \mathrm{d}r \qquad (2)$$

dx.doi.org/10.1021/ct300253n | J. Chem. Theory Comput. 2012, 8, 3536−3541

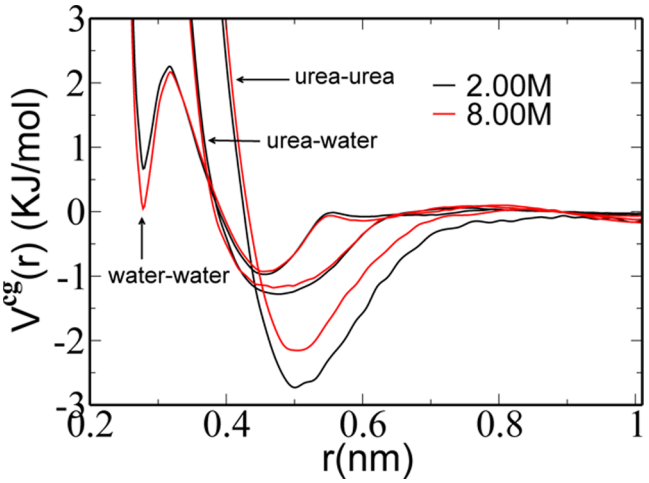

Figure 2. Coarse-grained potential $V^{cg}(r)$ for two different molar concentrations of urea.

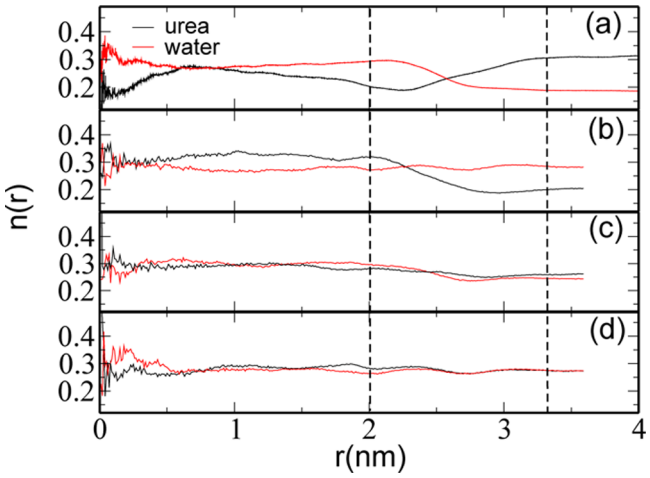

Figure 3. Normalized number density profile of urea $n(r)$ as a function of the distance from the center of the AdResS simulation domain for 8.02 M aqueous urea. (a) Initial density profile after a 20-ns-long AdResS simulation run, (b) after the application of the thermodynamic force for seven iterations only to the water molecules, and (c) followed by seven other iterations of the thermodynamic force for urea molecules, and (d) finally the thermodynamic force is applied to both components in the alternative steps to make a globally flat density profile. The hybrid region is situated between the two vertical dashed lines.

where averages in the grand canonical ensemble are denoted by brackets $\langle\cdot\rangle$, V is the volume, N_i is the number of particles of species "i" within the explicit region, δ_{ij} is the Kronecker delta, $g_{ij}^{\mu VT}(r)$ is the radial distribution function in the grand canonical (μVT) ensemble, and G_{ij}, the KBI, is a local quantity, which can be used as a measure of the affinity between solution components i and j. A positive (or negative) value of G_{ij} refers to an excess (or depletion) of component j around component i. In binary systems of cosolvent (c) and water (w), the link to the solvation thermodynamics is given by[34]

$$\gamma_{cc} = 1 + \left(\frac{\partial \ln \gamma_c}{\partial \ln \rho_c}\right)_{p,T} = \frac{1}{1 + \rho_c(G_{cc} - G_{cw})} \tag{3}$$

where γ_c is the molar cosolvent activity coefficient and $k_B T \ln \gamma_c$ is the cosolvent solvation free energy (at pressure p, temperature T, and cosolvent number density ρ_c). Similar expressions have been derived for systems that have a solute (s) at infinite dilution ($\rho_s \to 0$) in a cosolvent−water solution. In this case, the solvation free energy of the solute ($\Delta\mathcal{G}_s$) varies with the solution composition according to[34]

$$\lim_{\rho_s \to 0}\left(\frac{\partial \Delta\mathcal{G}_s}{\partial x_c}\right)_{p,T} = \frac{RT(\rho_w + \rho_c)^2}{\eta}(G_{sw} - G_{sc}) \tag{4}$$

where x_c is the cosolvent mole fraction, R is the gas constant, $\eta = \rho_w + \rho_c + \rho_w\rho_c(G_{ww} + G_{cc} - 2G_{cw})$, and ρ is the number density of individual components of the aqueous solutions. G_{ij} values are separately calculated for every cosolvent concentration in a pure water−cosolvent mixture. Preferential solvation of the solute by cosolvent molecules ($G_{sw} - G_{sc} < 0$) results in a decrease of $\Delta\mathcal{G}_s$ upon increasing the cosolvent mole fraction x_c or urea molar concentration c_c (salting-in). In our study, we will use urea as a cosolvent and a single triglycine as a solute.

3. RESULTS AND DISCUSSIONS

We perform AdResS simulations using the setup presented in Figure 1. We choose the size of the explicit (all-atom) region to have a 2 nm radius and the hybrid region to have a width of 1.3 nm. The cutoff for the interactions is set to 1.2 nm so that particles in the explicit region do not directly interact with those in the coarse-grained region. A typical linear dimension of the simulation box is around 8 nm that consists of approximately 15 000 molecules for the full range of concentrations. Note that this specific system size is only valid as long as we solvate a small peptide, triglycine in this case. For large proteins, a much larger simulation domain would be needed to maintain solvent equilibrium, which is crucial to successfully use KB theory to derive thermodynamic properties.

3.1. Pure Aqueous Urea: Deriving Thermodynamic Force. We start our discussion by presenting results for pure aqueous urea mixtures. For this purpose, we run a 20-ns-long trajectory for the mixture within the AdResS setup. From the simulation trajectory, we calculate the normalized density profiles. The results are depicted in part a of Figure 3. It is evident that the coupling leads to unphysical density variations. The nonuniform density profile is predominantly due to the pressure difference between the all-atom and coarse-grained regions. Recently, it has been shown that the observed discrepancy can easily be rectified by applying an iterative thermodynamic force[19]

$$f_{th}^{n}(r) = f_{th}^{n-1}(r) - \frac{1}{\rho^2 \kappa_T}\nabla\rho^{n-1}(r) \tag{5}$$

which predominantly depends on the slope of the density profiles within the hybrid region (for a detailed methodological description and applications, see refs 17, 19, and 29). Here, κ_T is the isothermal compressibility of the solvent mixture. We have shown previously that eq 5 can be effectively applied to a mixture.[17] Here, however, we propose an improved protocol to derive the thermodynamic force. A closer inspection of the curves in part a of Figure 3 suggests that even though the pressure is always higher (for both components) in the coarse-grained region, the urea molecules are usually pushed out of the explicit region. This is because the pressure difference ΔP_{aa-cg}, between the all-atom and coarse-grained representations, is always higher for water molecules than urea. Therefore, water

dx.doi.org/10.1021/ct300253n | J. Chem. Theory Comput. 2012, 8, 3536−3541

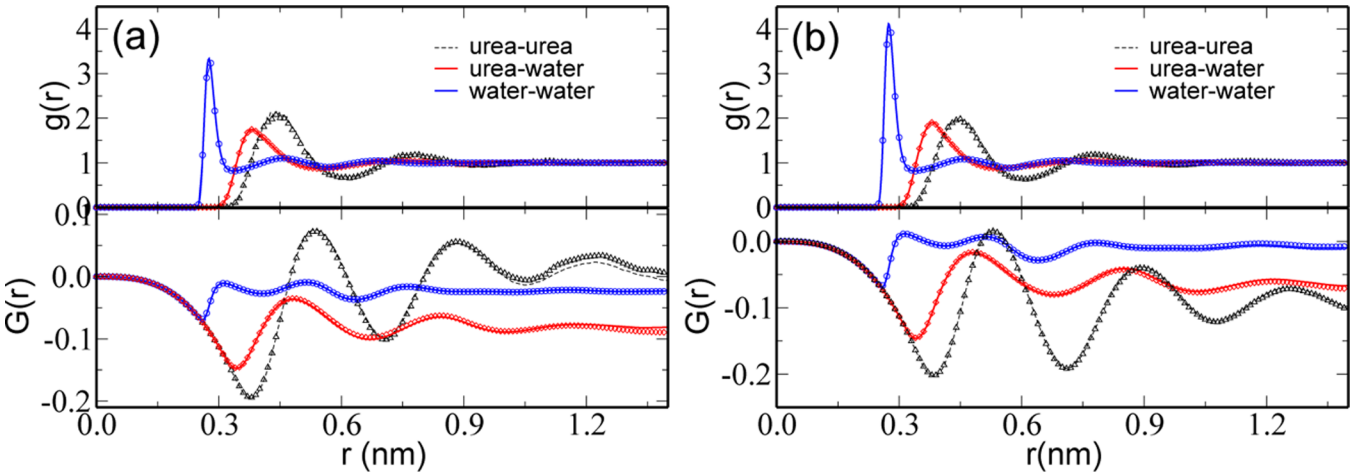

Figure 4. Radial distribution function $g(r)$ (top panel) and Kirkwood−Buff integrals $G(r)$ (bottom panel) for (a) 2.00 M and (b) 8.02 M aqueous urea solution. Results are shown for all three pairs. Lines are all-atom data, and symbols represent data from AdResS simulations that are calculated within the explicit region of 2 nm radius.

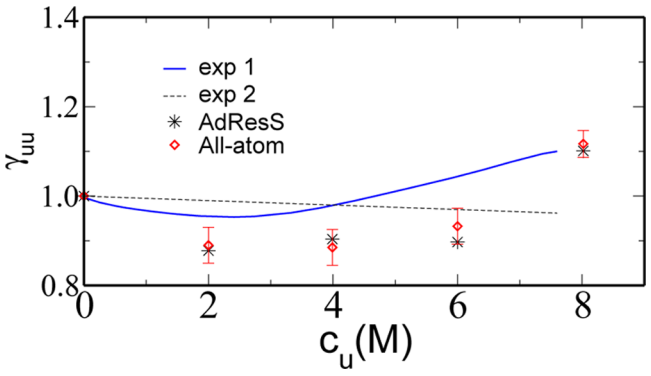

Figure 5. γ_{uu} as a function of urea molar concentration c_u (see eq 3). Error bars are standard deviations calculated out of six stochastically independent all-atom runs. The data set for exp 1 is taken from refs 25 and 35, and for exp 2, data are taken from ref 36.

molecules move preferentially into the explicit region rather than the urea, which finally affects the maximum particle packing density within the explicit region, leading to a reduced density of urea molecules inside the explicit region, as indicated in part a of Figure 3. Because of that, we adjust our protocol to derive the thermodynamic force for the mixtures at different concentrations. Here, we start by correcting the water molecule contribution until it reaches a flat density profile (see water density in the part b of Figure 3), which is done over seven iterations each with a 10-ns-long trajectory. This procedure leads to the drift of urea molecules from the coarse-grained to the all-atom region, and hence the density of urea molecules increases in the all-atom region, as reflected by the density profile of urea in part b of Figure 3. Afterward, we start correcting the urea density profile over another seven iterations, keeping the same thermodynamic force for water from the previous iteration. This correction is shown in the part c of Figure 3. A closer look at the plot reveals that this procedure produces a small drift in the water density profile. Therefore, in the final stages of correction, we apply eq 5 to the mixture with alternative iterations for another 40 iterations until the density profile of both components becomes flat. The final data are represented in the part d of Figure 3.

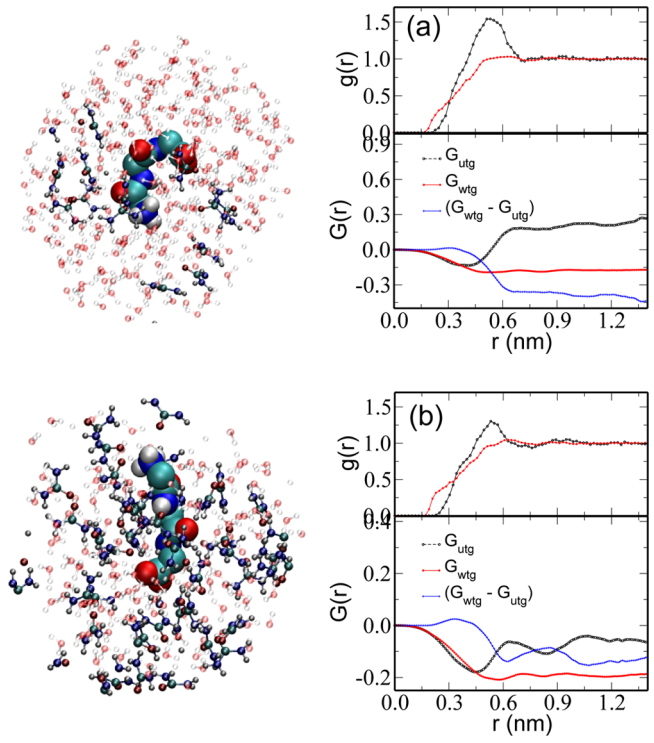

Figure 6. The radial distribution function g(r) and Kirkwood−Buff integral $G(r)$ for triglycine (peptide) solvated in the aqueous urea solutions for two different urea concentrations, (a) 2.00 M and (b) 8.02 M. The $g(r)$'s are calculated between the centers of mass of the individual molecules. Beside both graphs, we show the simulation snapshots of those molecules which are within 1 nm from the triglycine.

Once the flat density is observed within the full simulation domain, we calculate the KBI within the explicit region of the AdResS simulation. In Figure 4, we show $g(r)$'s and the corresponding KBIs between different pairs of the mixture for 2.00 and 8.02 M aqueous urea solutions. It can be appreciated that the results obtained from the AdResS simulations (symbols) are in good agreement with the all-atom data (lines). Furthermore, we have calculated KBIs for two more molar concentrations of urea, as indicated in the Methodology

dx.doi.org/10.1021/ct300253n | J. Chem. Theory Comput. 2012, 8, 3536−3541

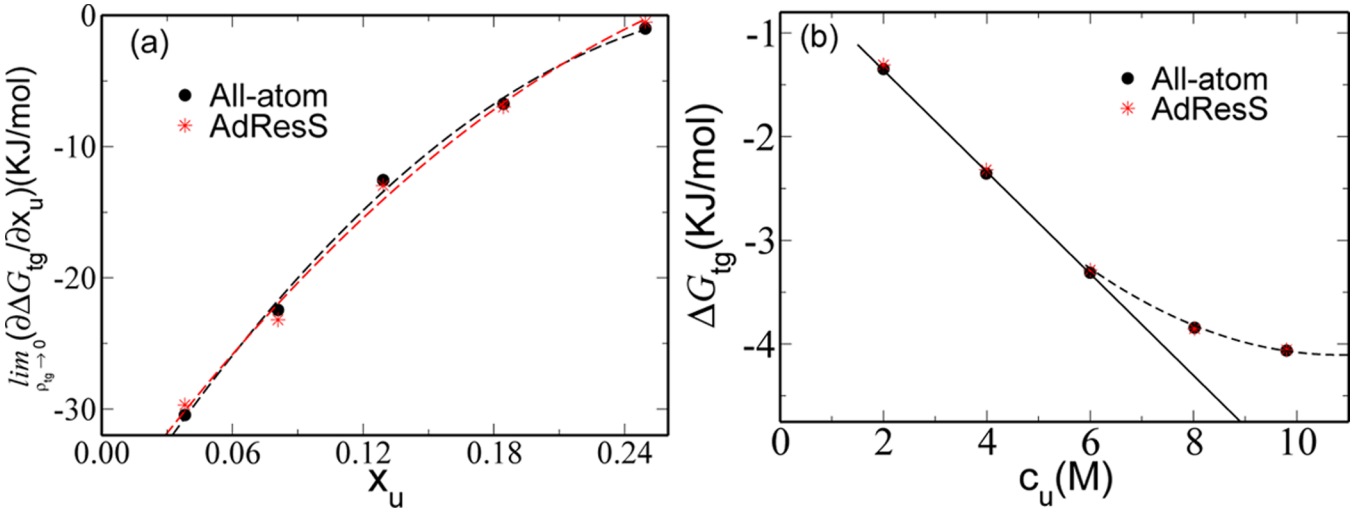

Figure 7. (a) Derivative of triglycine solvation free energy ($\partial\Delta\mathcal{G}_{tg}/\partial x_u$; see eq 4) as a function of the urea mole fraction x_u. Note: here, we use the urea mole fraction (instead of the urea molar concentration c_u) in the abscissa to be consistent with eq 4). So, the numerical integration can directly lead to solvation free energy $\Delta\mathcal{G}_{tg}$. (b) Solvation free energy $\Delta\mathcal{G}_{tg}$ as a function of molar concentrations c_u. Dashed lines are quadratic fits to the data in both main plots, with the color of the lines being consistent with the color of the symbol. The solid line in part b is a linear fit between 2 M and 6 M.

section. In those cases also, we find good agreement with the all-atom data (data not shown). Note that the integration limit r in eq 2 must be chosen sufficiently large such that $G_{ij}(r)$ converges to a plateau value, or oscillates in a well controlled way around a mean value. Here, we take the average between r = 0.9 nm and r = 1.4 nm to calculate the value of G_{ij}. This range is satisfactory, because $G_{ww}(r)$ and $G_{uw}(r)$ show a reasonable plateau, and $G_{uu}(r)$ oscillates around a mean within this range, see Figure 4.

A closer look at part a of Figure 4 shows a small discrepancy at the tail of the urea−urea KBI. This difference might look small at first glance. However, we want to point out that the calculation of thermodynamic properties using KB theory usually requires various combinations of the KBIs between the individual pairs of the aqueous cosolvent mixtures (see for example eqs 3 and 4). Thus, a small deviation in the KBI value may lead to a significant difference in the calculated thermodynamic properties. Therefore, in order to test the robustness of our approach in accurately representing the thermodynamic properties, we calculate γ_{uu} using eq 3. Results are shown in Figure 5. All-atom and AdResS data show excellent agreement over the full concentration range. For comparison, we also include experimental data. While the simulation data could not exactly reproduce experimental values, the trend follows very closely the first experimental data set of ref 35. This is a surprisingly close agreement, suggesting that the chosen force field properly captures interaction differences between urea and water over a significant concentration range. Furthermore, we also observe a speedup of up to three times by using AdResS over all-atom simulations. At first glance, this might appear to be small. However, in the case when the conformational transition of a large (bio)-macromolecule drives a large number of urea molecules toward the protein, a much larger surrounding osmotic reservoir is needed to maintain correct solvent equilibrium. Therefore, use of our approach will more significantly increase the computational efficiency.

3.2. Solvation Free Energy of Triglycine in Aqueous Urea. Having shown the results for aqueous urea solutions, we now focus on studying the solvation thermodynamics of triglycine in aqueous urea mixtures at different urea mole fractions. The radial distribution function $g(r)$ and corresponding KBIs $G(r)$ are given in Figure 6. The derivative of the solvation free energy $(\partial\Delta\mathcal{G}_s/\partial x_u)_{p,T}$ can be calculated using eq 4. As indicated, the solvation energy calculation requires triglycine/water and triglycine/urea KBIs, which are shown in Figure 6 for two different urea concentrations from AdResS simulations. We also include the difference $(G_{wtg} - G_{utg})$, which is directly related to the derivative of triglycine solvation free energy of eq 4. In part a of Figure 7, we show a comparative plot of $(\partial\Delta\mathcal{G}_s/\partial x_u)_{p,T}$ using all-atom and AdResS simulations. It is clear from the plot that the AdResS (or open boundary) scheme can effectively reproduce the generic (bio)physical behavior observed from a more computationally expensive all-atom simulation of the solvated triglycine. It is still important to mention that for all concentrations of urea, we observe salting-in (i.e., $(\partial\Delta\mathcal{G}_{tg}/\partial x_u)_{p,T} < 0$), suggesting the preferential interaction of urea with the triglycine over water. Furthermore, the trend of Figure 7a also suggests that $\Delta\mathcal{G}_{tg}$ decreases with increasing urea concentration (see Figure 7b), which is nothing but the preferred solvation of triglycine at higher urea concentrations. While the variation of $\Delta\mathcal{G}_{tg}$ with c_u usually follows linear dependence in experiments,[37] simulations usually observe a quadratic dependence.[8] Here, however, we observe a nice linear dependence for a $c_u \leq 6$ M urea concentration. For $c_u > 6$ M, $\Delta\mathcal{G}_{tg}$ deviates away from the linear dependence to somehow approach a plateau value (see Figure 7b). These observations are consistent with the known facts that the thermodynamic driving force, toward better solubility, is around 8.02 M urea[10,11] and thus leads to protein denaturation in aqueous urea solutions. Another quantity that can be derived from the Figure 7b is the m-value for peptide solvation, which is defined as

$$m\text{-value} = \frac{\partial\Delta\mathcal{G}_{tg}}{\partial c_u} \tag{6}$$

If we take the m-value (per residue) from the slope of the linear fit in Figure 7b, we find −0.164 kJ mol^{-2} L. This value is in a

dx.doi.org/10.1021/ct300253n | J. Chem. Theory Comput. 2012, 8, 3536−3541

close agreement with the experimental value of −0.163 kJ mol^{-2} L.[8,38] It is yet important to mention that the calculation of the *m*-value from the simulations assumes equal contribution of each residue of a triglycine,[8] which is reasonable as long as we choose a peptide with only a few amino acids. Therefore, our new open boundary simulation approach, applied to a simple test case of triglycine, could capture all the necessary ingredients of the solvation thermodynamics of the more complex bio(macro)molecules.

4. CONCLUSIONS

We present a systematic analysis of the solvation of a peptide (triglycine), at room temperature T = 300 K, in aqueous urea mixtures in an "effective" open boundary molecular dynamics approach, which allows one to reduce the computational cost significantly. The work is based on the fluctuation theory for solutions derived by Kirkwood and Buff for open systems. We have calculated the derivative of the urea molar activity coefficient and the derivative of the triglycine solvation free energy. The results from the open boundary simulations are found to be in good agreement with the all-atom data and also with the existing experiments. Though we here only tested a triglycine in the aqueous urea solutions, this approach can possibly be further used to study the concentration driven conformational transition of more complex (bio)-macromolecules.

AUTHOR INFORMATION

Corresponding Author

*E-mail: kremer@mpip-mainz.mpg.de.

Notes

The authors declare no competing financial interest.

ACKNOWLEDGMENTS

D.M. thanks Christine Peter and Christoph Globisch for many stimulating discussions and Christine Peter for pointing out some relevant literature in the field. We thank Jia-Wei Shen, Karen Johnston, and Raffaello Potestio for critical reading of the manuscript. Snapshots in this manuscript are rendered using VMD.[39]

DEDICATION

This work is dedicated to Wilfred van Gunsteren on the occasion of his 65th birthday in appreciation of his scientific accomplishments and his achievements as an academic teacher.

REFERENCES

(1) Kauzmann, W. *Adv. Protein Chem.* **1959**, *14*, 1−63.
(2) Wyman, J. *Adv. Protein Chem.* **1964**, *19*, 223−286.
(3) Ben-Naim, A. *J. Phys. Chem.* **1967**, *71*, 4002−4007.
(4) Dill, K. *Biochemistry* **1990**, *29*, 7133−7155.
(5) Record, M. T.; Zhang, W. T.; Anderson, C. F. *Adv. Protein Chem.* **1998**, *51*, 281−353.
(6) van der Vegt, N. F. A.; van Gunsteren, W. F. *J. Phys. Chem. B* **2004**, *108*, 1056−1064.
(7) Ma, L.; Pegram, L.; Record, M. T.; Cui, Q. *Biochemistry* **2010**, *49*, 1954−1962.
(8) Horinek, D.; Netz, R. R. *J. Phys. Chem. A* **2011**, *115*, 6125−6136.
(9) Guinn, E. J.; Pegram, L. M.; Capp, M. W.; Pollock, M. N.; Record, M. T., Jr *Proc. Natl. Acad. Sci.* **2011**, *108*, 16932−16937.
(10) Afinsen, C. B. *Science* **1973**, *181*, 223−230.
(11) Bennion, B. J.; Daggett, V. *Proc. Natl. Acad. Sci.* **2003**, *100*, 5142−5147.
(12) Mountain, R. D.; Thirumalai, D. *J. Am. Chem. Soc.* **2003**, *125*, 1950−1957.
(13) Stumpe, M. C.; Grubmüller. *Plos Comput. Biol.* **2008**, *4*, e1000211−10.
(14) Gattin, Z.; Riniker, S.; Hore, P. J.; Mok, K. H.; van Gunsteren, W. F. *Protein Sci.* **2009**, *18*, 2090−2099.
(15) Berteotti, A.; Barducci, A.; Parrinello, M. *J. Am. Chem. Soc.* **2011**, *133*, 17200−17206.
(16) Zhou, R.; Li, J.; Hua, L.; Yang, Z.; Berne, B. J. *J. Phys. Chem. B* **2011**, *115*, 1323−1326.
(17) Mukherji, D.; van der Vegt, N. F. A.; Kremer, K.; Delle Site, L. *J. Chem. Theory Comput.* **2012**, *8*, 375−379.
(18) Praprotnik, M.; Poblete, S.; Kremer, K. *J. Stat. Phys.* **2011**, *145*, 946−966.
(19) Fritsch, S.; Poblete, S.; Junghans, C.; Delle Site, L.; Ciccotti, G.; Kremer, K. *Phys. Rev. Lett.* **2012**, *108*, 170602−5.
(20) Praprotnik, M.; Delle Site, L.; Kremer, K. *J. Chem. Phys.* **2005**, *123*, 224106−14.
(21) Praprotnik, M.; Delle Site, L.; Kremer, K. *Annu. Rev. Phys. Chem.* **2008**, *59*, 545−571.
(22) Poblete, S.; Praprotnik, M.; Kremer, K.; Delle Site, L. *J. Chem. Phys.* **2010**, *132*, 114101−7.
(23) Kirkwood, J. G.; Buff, F. P. *J. Chem. Phys.* **1951**, *19*, 774−777.
(24) Lindahl, E.; Hess, B.; van der Spoel, D. *J. Mol. Mod.* **2001**, *7*, 306−317.
(25) Weerasinghe, S.; Smith, P. E. *J. Phys. Chem. B* **2003**, *107*, 3891−3898.
(26) Berendsen, H. J. C.; Grigera, J. R.; Straatsma, T. P. *J. Phys. Chem.* **1987**, *91*, 6269−6271.
(27) van Gunsteren, W. F.; Billeter, S. R.; Eising, A. A.; Hünenberger, P. H.; Krüger, P.; Mark, A. E.; Scott, W. R. P.; Tironi, I. G. *Gromos43a1*; Hochschulverlag AG an der ETH Zürich, Zürich Switzerland, 1996.
(28) Berendsen, H. J. C.; Postma, J. P. M.; van Gunsteren, W. F.; DiNola, A.; Haak, J. R. *J. Chem. Phys.* **1984**, *81*, 3684−3690.
(29) Fritsch, S.; Junghans, C.; Kremer, K. *J. Chem. Theory Comput.* **2012**, *8*, 398403.
(30) Praprotnik, M.; Matysiak, S.; Delle Site, L.; Kremer, K.; Clementi, C. *J. Phys. Condens. Mater.* **2007**, *19*, 292201−10.
(31) Reaction field dielectric constants are taken from PME treated all-atom simulations. The values are ε_r = 70 for 2.00 M urea, 68 for 3.99 M urea, 67 for 6.00 M urea, and 69 for 8.02 M urea.
(32) Hess, B.; Bekker, H.; Berendsen, H. J. C.; Fraaije, J. G. E. M. *J. Comput. Chem.* **1997**, *18*, 1463−1472.
(33) Rühle, V.; Junghans, C.; Lukyanov, A.; Kremer, K.; Andrienko, D. *J. Chem. Theory Comput.* **2009**, *5*, 3211−3223.
(34) Ben-Naim, A. *Molecular Theory of Solutions*; Oxford University Press: New York, 2006.
(35) Stokes, R. H. *Aust. J. Chem.* **1967**, *20*, 20872100.
(36) Miyawaki, O.; Saito, A.; Matsuo, T.; Nakamura, K. *Biosci. Biotechnol. Biochem.* **1997**, *61*, 466469.
(37) Makhatadze, G. I. *J. Phys. Chem. B* **1999**, *103*, 4781−4785.
(38) Auton, M.; Wayne Bolen, D. *Proc. Natl. Acad. Sci.* **2005**, *102*, 15065−15068.
(39) Humphrey, W.; Dalke, A.; Schulten, K. *J. Mol. Graphics* **1996**, *14*, 33−38.